

Erosion after an extreme storm event in an arid fluvial system of the southern Atacama Desert: an assessment of magnitude, return time, and conditioning factors of erosion and debris flows generation

Germán Aguilar¹, Albert Cabré^{1,2}, Víctor Fredes^{1,3}, and Bruno Villela^{1,3}

¹Advanced Mining Technology Center, Facultad de Ciencias Físicas y Matemáticas, Universidad de Chile, Avenida Tupper 2007, Santiago, Chile

²Departamento de Ciencias Geológicas, Universidad Católica del Norte, Avenida Angamos 0610, Antofagasta, Chile

³Departamento de Geología, Facultad de Ciencias Físicas y Matemáticas, Universidad de Chile, Plaza Ercilla 803, Santiago, Chile

Correspondence: Germán Aguilar (german.aguilar@amtc.cl)

Abstract. We have calculated a mean erosion of 1.3 mm caused by an individual storm event in March 2015 that impacted a large mountainous area of the southernmost Atacama Desert. The calculated erosion agrees with millennial erosion rates and with return time of high sediment discharge events previously reported in the study area. Here, we quantify for the first time the contribution of an individual extreme storm event to long-term erosion rates in the Atacama Desert. This is significant because erosion rates, related to high sediment discharge events in arid fluvial systems, are hard to measure with sediment load due the destruction of gauges by devastating flashfloods and thus have not been directly measured yet. During the March 2015 storm, debris flows were reported as the main sediment transport process. Erosion of gullies and channels are the main source of sediments that finally generate debris flows that reach the tributary junctions and the trunk valleys. The sediment yield to the tributary outlets strongly depends on the hydraulic capacity of catchments to store sediments in the drainage network between storms. Larger tributary catchments, high hydrological hierarchy, low topographic gradient and gentle slopes are the most susceptible catchments to generate debris flows that reach alluvial fans at any storm event from large debris volumes stored in the drainage network. Our findings better assess debris flow susceptibility of arid catchments, which is significant for the southernmost Atacama Desert valleys because human settlements and industries are mostly established on alluvial fans.

Copyright statement. TEXT

15 1 Introduction

The hydrology of the Atacama Desert is characterized by rivers that flow from the high Andean mountain ranges fed from snow, glaciers and permafrost melting (Favier et al., 2009; Gascoïn et al., 2011). In this scenario, the presence of perennial rivers is restricted to the trunk valleys whilst tributary valleys of the mid-mountainous region and of the Andean foothills host ephemeral streams. High runoff and sediment discharge in these fluvial systems is triggered by intense rare rainfall events. The

influence of extreme storms has resulted in important runoff erosive events in the past recorded by coarser grain size layers in both lacustrine and marine archives during the last 5,500 years in the Atacama Desert (Ortlieb, 1994, 1995; Veit, 1996; Rein et al., 2005; Maldonado and Villagrán, 2006; Vargas et al., 2006; Martel-Cea et al., 2016; Tiner et al., 2018; Ortega et al., 2012, 2019). The return time of extreme runoff erosive events decreased from 1 event/210 yrs. to 1 event/ 40 yrs. during the last 5 1000 yr. This is interpreted as an intensification of ENSO storms activity in Northern Chile (Ortega et al. (2019) and references therein).

The Atacama Desert has been impacted historically by extreme storm events that usually occur during southern hemisphere winters. Almost all the available records are from local newspapers and have been recently compiled in Ortega et al. (2019); Vargas et al. (2018). Most of the events triggered flash floods and landslides that affected preferred sites for human settlements 10 such as fluvial plains and alluvial fans. Catastrophic slope processes, including debris flows, caused human casualties and considerable economic loss in the main towns situated at El Salado River, El Copiapó River, El Huasco River and El Elqui River. In March 2015 a storm impacted a large area of the Atacama Desert (Barret et al., 2016; Wilcox et al., 2016; Bozkurt et al., 2016; Jordan et al., 2019). This event occurred during southern hemisphere summer in an area where the higher mountain ranges (above 3500 m a.s.l.) usually experience precipitation as snow. The high elevation of the zero-isotherm during the March 15 2015 event caused erosion in areas where usually snow delays and slows run-off (Wilcox et al., 2016; Jordan et al., 2019) .

Extreme storm events greatly contribute to erosion in arid zones (Tarr, 1890; Coppus and Imeson, 2002). This influence has been highlighted in Carretier et al. (2018) in the Andean catchments of Chile. This is reinforced by Terrestrial Cosmogenic Nuclides differences in the concentration in sediments supplied by landslides or debris flows against sediments supplied by the combination of fluvial processes in El Huasco river valley (Aguilar et al., 2014) and for others (semi)arid fluvial systems 20 of Chile (Carretier et al., 2015). Therefore, erosion magnitude and distribution after extreme storms is of major interest for both landscape evolution modelling and sediment cascades analysis in the southernmost Atacama Desert. However, the precise quantification of catchment erosion during a major flood event has not yet been established. This might be explained because of the lack of high-resolution digital elevation models (e.g. Lidar point clouds in Anderson et al. (2015)) and by the absence of available detailed topography for the Atacama Desert. The problem is compounded the lack or scarcity of meteorological and 25 fluviometric stations suitable to measure hourly-rain intensity and sediment load yielding, respectively.

The aim of this study consists of evaluating the erosion during the March 2015 storm in catchments of El Huasco river valley (Fig. 1). We have calculated the erosion within tributary catchments (whole area of 1,500 km²) based on volumes of debris flow deposits measured in tributary junction alluvial fans after the storm. The calculated erosion agrees with the Holocene erosion rates presented in Aguilar et al. (2014) by concentrations of Terrestrial Cosmogenic Nuclides in stream 30 sediments. Thus, we illustrate how the erosion in this arid area is dictated by the repetition of extreme individual storm events such as the March 2015 event. Furthermore, the statistical evaluation proves that the topographic attributes of the catchment enhance debris-storage within the catchments are significant to debris flow generation. These results suggest that debris-storage below the zero-isotherm altitude should be considered to properly define the susceptibility to debris flow generation within the catchments, and these are significant to Hydrometeorological hazards assessment.

2 Study area

El Huasco river valley is one of the main fluvial systems in the climatic transition area between the hyper-arid core of the Atacama Desert and the semiarid region of the Central Chile. This watershed has two main rivers: El Carmen River and El Tránsito River. These two rivers have permanent runoff from snow and permafrost melting from the higher tributaries.

5 Currently glacial and periglacial environment are present above 4000 m a.s.l. and Late Pleistocene glacial evidences are not present below 3200 m a.s.l. (Aguilar, 2010).

The mid-mountainous zone of this fluvial system situated between 3500-1000 m a.s.l. (Fig. 1), is usually impacted by spatially heterogeneous extreme storm events which trigger shallow landslides and debris flows in the tributary catchments. The episodic sedimentation associated to individual storm events is recorded in the Holocene stratigraphic arrangements in
10 some of the tributary-junction alluvial fans (Veit, 1996; Aguilar, 2010; Cabré et al., 2017, 2019). Authors identified a number of cohesive debris flows in different alluvial fans indicating the episodic nature of sedimentation whereas gravel-sheet couplets and open framework gravels indicate more continuous sedimentation in the alluvial fans associated to relatively more humid periods within the Holocene (Cabré et al., 2019).

The quantification and characterization of erosion and sedimentation in the Huasco river valley has been interpreted by
15 different authors as a climatic and tectonic induced signal (Aguilar et al., 2011, 2013, 2014; Rossel et al., 2018). At a 10^6 -year time-scale, tectonic and climatic factors which combines the aridization and the Andean uplift are coupled to develop a transient landscape organization (Aguilar et al., 2013). The calculated mean erosion rates of 0.03-0.08 mm/yr during the last 10-6 Ma not reach the fully degradation of the Miocene surfaces situated at the highest altitudes (Aguilar et al., 2011). Millennial erosion rates (10^4 -year) measured by means of Terrestrial Cosmogenic Nuclides concentrations in the river sediments agree
20 with 10^6 -year time-scale erosion rates (Aguilar et al., 2014).

Permo-Triassic igneous-metamorphic and Mesozoic rocks are exhumed during the Cenozoic and represent the highest mountain ranges in the area. The bedrock is dominated by Permo-Triassic igneous-metamorphic rocks which are subdivided based on Salazar et al. (2013) into: Pampa Gneiss, Tránsito Metamorphic Complex and Chancoquín Plutonic Complex. Mesozoic Volcano-sedimentary units are also present between these Permo-Triassic rock-blocks: San Félix Fm., Lautaro Fm., and Lagunillas Fm. These lithological units have been intruded by several Cenozoic plutons and are overlain by Cenozoic unconsolidated
25 gravel deposits (e.g. Atacama Gravels) and volcanic deposits (Salazar et al., 2013).

Five geological groups were defined by Fredes (2016) considering a rock strength classification (González de Vallejo, 2002) of the geological units of Salazar et al. (2013) (Fig. 9a). Geo1 corresponds to intrusive rocks, Geo2 corresponds to volcanic and coarse-sedimentary rocks, Geo3 corresponds to metamorphic rocks, Geo4 corresponds to fine grained rocks (shales and
30 siltstones) and Geo5 corresponds to unconsolidated Pleistocene-Holocene deposits. This strategy and the measurement of Schmidt hammer values has been applied in the Morocco Atlas by Stokes and Mather (2015) to characterize the lithological influence in the debris flows generation.

3 Methods

Immediately after the March 2015 storm we performed a field survey in El Huasco river valley. We observed (1) debris flow deposition on the alluvial fan surfaces and (2) alluvial fan formation in the confluence of the tributary with the trunk valley. Analysis of deposits showed different rheologies of Debris flows ranging from cohesive debris flows and hyper-concentrated flows to mud flows. Here, to simplify the statistical analysis we do not differentiate between flow-types and henceforth we will include all under the “debris flow” term sensu stricto. For details on the spatial and temporal distribution of debris flows pulses in the fans, readers are referred to Cabré et al. (submitted).

We have calculated the mean erosion (mean landsurface lowering in millimeters) after the March 2015 storm event for each of the tributary catchments and for the whole catchments within the study area with the debris flow deposits volumes (Fig. 1, tributaries inside dashed-line white box). Tributary catchment were extracted use of a Geographic Information System. The Digital Elevation Model is provided by NASA/JPL-Caltech with a nominal spatial pixel resolution of 30 x 30m (<https://asterweb.jpl.nasa.gov/gdem.asp>) and a nominal vertical resolution of 1.0 m.

The volumes of debris flow deposits were estimated using equation 1. This equation calculates the volume of fans by assuming a simplistic conical geometry and is adapted from the Campbell and Church (2003) equation for colluvial fan volume calculations.

$$Volume = \left(\frac{wlt}{2}\right) \frac{\pi}{3} \quad (1)$$

Width (w) and thickness (t) of fan toes were measured in the field with a measuring tape for 16 alluvial fans, whereas their axial length (l) was measured on the available satellite imagery. Width and length for the rest of the fans (33) was measured from RapidEye images. Based on the fieldwork measurements, a thickness of one meter was considered for the fans whose length and width were measured on RapidEye images. The volumes have been corrected with a bulking factor which considers a porosity value of 30% (Nicoletti and Sorriso-Valvo, 1991).

We have characterized the erosion processes within catchments from both fieldwork observations and the analysis of optical satellite imagery retrieved from Planet Team (2017). The available images of 3m/pixel for Planet Scope imagery and 6.5m/pixel for RapidEye imagery does not assist in the identification of rills and small gullies. Thus, field observations are crucial to identify these erosion indicators.

Topographic attributes of catchments were selected in order to analyze their influence on debris flow generation and erosion processes after the March 2015 storm. In order to characterize the tributary catchments, the topographic attributes were selected based on their influence on different processes such as peak flow generation and debris storage (Strahler, 1958; Melton, 1965; Howard and Kerby, 1983; Wilford et al., 2004): Area, Length (straight-line between outlet and head-water of tributary catchments), Maximum elevation, Gradient (inclination of length), Average Slope, Gravelius index (Shape), Hypsometry, Melton ratio (index of roughness that normalizes relief by area; Melton (1957)), Drainage density, maximum Strahler order, concavity, and steepness index of the main thalweg.

A statistical analysis was calculated in order to find outliers or anomalies in the topographic attributes that might control debris flow generation in tributary catchments. The significance of each attribute in debris flows generation is determined by an Analysis of variance (ANOVA). The ANOVA determines if the mean values are similar between the catchment classes that generated debris flows against catchments that did not generate debris flows. The proposed tests consisted in splitting the total data variance into several components (between groups and within groups) and in comparing these components with a Fisher mean test with a critical value of 0.05 (Box et al., 1978; Davis, 2002). Principal Components Analysis (PCA) was performed to group the variables related to debris flow generation in common factors that might explain the variance of the catchments attributes, reducing the number of variables and providing a weighting factor for each attribute within the group (Levy and Varela, 2003). A normalized classification of catchment-clustering was performed by the weighted mean of the attributes that control the debris flow generation on each catchment.

Geological groups were defined in order to analyze the influence of the rock units on the debris-flow generation based on the map of Salazar et al. (2013). Eight hundred and forty Schmidt Hammer (SH) rebound values were measured in little-weathered bedrock outcrops in 41 selected field stations to provide a rock strength classification of the geological groups as similarly presented in Stokes and Mather (2015) for tributary catchments in Morocco. We did not measure unconsolidated sediments because SH values are below instrumental detection ($SH < 10$) (Selby, 1993). The rock strength classification includes more than 100 measurements for each of the geological groups. Additionally, a statistical analysis was performed for each geological group. Finally, we calculated the normalized SH values for the catchments considering areal percentage of the geological groups, Mean Schmidt Hammer values (MeanSHn) and IQR Schmidt Hammer values (IQRSHn). The MeanSHn values represent a little-weathered-rock strength index for the catchments whilst IQRSHn values represent an index of the weathering and cracking status of the bedrock as suggested in Roda-Boluda et al. (2018).

4 Results

4.1 Erosion processes during the storm event

Hillslopes of El Huasco river tributary catchments were impacted by a combination of water erosion processes during the March 23rd-26th 2015 storm. In which amongst all, erosion of the upper mantled-hillslopes layer occurred when water concentrated and formed rills or gullies (Fig. 2 and Fig. 3). Rills start to form by overland flow when a critical shear stress is reached (Horton, 1945). If overland flow meets bare hillslopes characteristically of arid zones, hillslope erosion occurs at any mean-average storm because of the high erodibility of the upper soil layer. On the other hand, narrow and deep channels (gullies) are relatively permanent in hillslopes and usually allow the transmission of water and sediment from upper hillslope areas towards the main drainage network within catchments.

The March 2015 storm event severely impacted the alluvial channels of the drainage network that store large volumes of sediment within tributary catchments (Fig. 2b). The entrainment of sediments resulted in different pulses of debris flows with different sediment to water ratios. Debris flows were followed by a strong incision that facilitated sediment transport

from alluviated channels downsystem. When these debris flows lost confinement at the outlet of the tributary catchments their deposition occurred (Fig. 2fg).

Gravitational landslides and rockslides of hillslopes are the main sediment sources that characteristically fill alluvial channels within storm periods and after storm events. The large volume of sediments is enhanced by the low-frequency of extreme storm events that usually impact the area. Hence, the return time of extreme storm events in this arid zone ranges from 1 event/ 200 years to 1 event/ 40 years (Ortega et al. (2019) and references therein) facilitates the storage of sediments in inter-storm periods and thus prepare these channels to yield sediment downsystem at any extreme storm event that impacts the area. This geomorphological 'behaviour' is known in the literature as transport-limited catchments (Bovis and Jakob, 1999) and is characteristic of arid landscapes.

10 4.2 Debris flows volumes and mean erosion

Debris flows that reached the tributary junctions with the trunk valley and produced deposit greater to 500 m³ of sediment during the March 2015 event were reported in forty-nine of one hundred twenty-four catchments (Fig. 4). The remaining seventy-five catchments did not yield debris flows deposits greater to 500 m³ of sediments in the tributary junctions. The volumes of the debris flow deposits vary between 530 and 234,000 m³. The mean erosion values (mean landsurface lowering) for the tributary catchments obtained from the calculated volumes of debris flow deposits that reached the alluvial fans vary between 0.3 and 35 mm (Fig. 4). The propagation of errors entails an uncertainty of 10% for the volumes calculated with field measurements and 40% for volumes estimated by satellite image measurements. The total sediment yield by debris flows to the tributary junction alluvial fans is approximately 1 million m³. If we consider the total area of tributary catchments (including the catchments where debris flow were absent in the tributary junctions) the total average erosion reported for the extreme storm event of March 2015 is 1.3 mm.

4.3 Catchment topographic attributes

Topographic attribute values for all tributary catchments and statistical analysis is available in supplementary data. Six topographic attributes (Area, Length, Strahler Order, Slope, Melton ratio and Relief ratio) proved to be significant in the debris flow generation, with a level of significance below 0.05 in the ANOVA. Two groups resulted from the PCA and each includes three topographic attributes. Group 1 integrates the catchment size and the hydrological hierarchy of the drainage network which includes: Area (A), Length (L) and Strahler order (O). Group 2 integrates the catchment relief and includes Average Slope (S), Gradient (G) and Melton ratio (M). From these two groups, two conditioning-factors were calculated: Size Factor and Relief Factor. These factors correspond to a linear combination of the attributes resultant from the PCA and the weighting of each attribute set by its weight. Therefore, two conditioning-factor values resulted from the addition of three normalized values of attributes (X_n) weighted by the weighting factor calculated by the PCA.

$$SizeFactor = (A_n * 0.92) + (L_n * 0.90) + (O_n * 0.89) \quad (2)$$

$$\text{Relief Factor} = (Sn * 0.95) + (Gn * 0.80) + (Mn * 0.70) \quad (3)$$

Size Factor and Relief Factor show an inverse correlation for catchments that generated debris flows and for catchments where clean water flows flushed downsystem in the tributary junctions (without debris flows generation) (Fig. 5a). The inverse correlation is also observed in the percentage of catchments with different range of factors, because the percentage of catchments that generated debris flows in the tributary junctions increases with Size Factor while it decreases with Relief Factor (Fig. 6ab). In fact, debris flows were present only in 18% of very small and low hierarchical catchments (low values of Size Factor, 0.05-0.25). In contrast, debris flows were present in 57% of large and high hierarchical catchments (high values of Size Factor, 0.75-1.50). Debris flows occurred only in 9% of the catchments with high mean slope values and high topographic gradient (high-Relief Factor, 1.75-2.00) whilst in 50% of the catchments with low slope values and low topographic gradients, debris flow occurred (low-Relief Factor, 0.25-1.25). These results suggest that debris flows were generated in the tributary junctions from larger and more hierarchical catchments with low topographic gradients and low mean slopes, whereas from smaller and steeper catchments debris flow were sparsely generated (Table 1).

The six topographic attributes (Area, Length, Strahler Order, Average Slope, Gradient, and Melton ratio) considered in the two conditioning-factors are reclassified to 0, 1 and 2 depending on the percentage of catchments favorable to debris flow generation. Finally, the weighting factor calculated by the PCA resulted in a normalized catchments-clustering. This catchments-clustering is added in a geographic information systems and resultant in a map of susceptibility (Fig. 7).

Size Factor and Relief Factor also show a correlation with volumes of debris flow deposits (Fig. 8ab). Volumes of sediment smaller than 6,000 m³ were supplied from small and low-hierarchical catchments (low values of Size Factor, minor than 0.25), whereas from large and high hierarchical catchments (high values of Size Factor, greater than 0.75) volumes were higher than 6,000 m³. On the other hand, sediment supply was smaller in catchments with high mean slopes values and high topographic gradients (high-Relief Factor, greater than 1.75) rather than in catchments with low slopes values and low topographic gradients (low-Relief Factor, minor than 1.25). Therefore, topographic attributes involved in the both conditioning-factor are also significant for debris flow deposit volumes.

25 4.4 Catchment lithological attributes

One hundred sixty Schmidt Hammer (SH) rebound values were measured in Geo1, 240 in Geo2, 280 in Geo3 and 160 in Geo4. Data outside the standard deviation in each station was excluded in order to remove data that could be affected by operator handling errors. Whisker and box plots show the distribution values for each geological group (Fig. 9b). The values of the 50-percentile (Q2) and the interquartile range (IQR=Q3 - Q1) represent the dispersion of values between 75 and 25 percentiles. We used the normalized values of the Mean Schmidt Hammer (MeanSHn) and the Interquartile Range of Schmidt Hammer (IQRSHn) in order to evaluate the strength of the unaltered rocks and the weathering degree of the rocks within the catchments.

MeanSHn and IQRSHn resulted from the addition of SH mean and SH IQR values for each geological group weighted by its areal percentage for each catchment (GeoX).

$$MeanSHn = (Geo1 * 43) + (Geo2 * 49) + (Geo3 * 41) + (Geo4 * 25) + (Geo5 * 10) \quad (4)$$

$$IQRSHn = (Geo1 * 8) + (Geo2 * 6) + (Geo3 * 10) + (Geo4 * 10) + (Geo5 * 1) \quad (5)$$

MeanSHn and IQRSHn present a weak correlation in both catchment' types (catchments that generated debris flows and which not) (Fig. 5b). Additionally, no correlation emerged between MeanSHn-IQRSHn and Size-Relief Factors (Fig. 5c-f). The percentage of catchments generating debris flows does not vary significantly in relation to the range of MeanSHn and IQRSHn (Fig. 6cd). The latter suggests that unaltered-rock strength represented by MeanSHn and weathering degree or fracturing degree of rocks represented by IQRSHn of geological units is not significant in debris flows generation for catchments impacted by the March 2015 storm event. Moreover, MeanSHn and IQRSHn do not exhibit a clear correlation with the volumes of debris flow deposits (Fig. 8cd).

5 Discussion

5.1 Conditioning-factors for debris flows generation

Debris flows, hyper-concentrated flows and mud flows in arid and semiarid Andes of northern Chile during intense rainfalls are usually linked to an increase in the pore pressure of the surficial loose debris layer generating a shallow-slide in the hillslopes of catchments (e.g., Sepúlveda and Padilla, 2008). Rock strength determines weathering rates and controls grain-size supply which finally dictates the production rate of debris to the hillslopes. However, rock strength does not determine the selective debris flow generation in the catchments during the March 2015 storm in El Huasco river valley. We propose based on field observations that this is because debris supply from rocky outcrops of hillslopes is not a significant source of sediments during the storms. Instead, we propose that the main source of debris flows is sediment stored in the drainage network.

Recent studies of debris flow generation assessment show that shallow debris-mantled hillslope failures is not required to trigger debris flows in arid catchments during intense and low frequency storm events (Vergara et al., 2018). Hillslope stability is favored by the transport-limited conditions characteristic of arid catchments. Furthermore, transport limited condition favor the storage of sediment in the alluvial channels, where debris entrainment to tributary junction alluvial fans by run-off from alluvial channels can occur at any storm that affects the area (Coe et al., 2008; Kean et al., 2013). The latter agrees with our field evidence that considers the available debris in the alluvial channels as the main entrainment source areas of sediment that were able to generate debris flows during the March 2015 storm event in El Huasco river valley. In that sense, similar interpretations were deduced based on field observations in catchments situated 300 km north of the study area, where flashfloods were

reported as the main erosion agents in the alluvial channels whereas hillslopes remained surprisingly stable during the March 2015 storm event (Wilcox et al., 2016).

Landslides on debris-mantled hillslopes are related to short and high intensity rainfall events (e.g., Coppus and Imeson, 2002; Berti et al., 2012). Rainfall thresholds responsible for triggering landslides have been proposed after inventories were
5 taken in monsoon impacted zones with the greatest reported rainfall intensities worldwide (e.g. Marc et al., 2018), and rainfalls of southern Chile that exceed the accumulated rainfall during the March 2015 event in the Atacama Desert by ten times (Jordan et al., 2019). In El Huasco river valley, landslides in hillslopes were scarce and certainly not the main erosion process (Cabr e et al., submitted). Conversely, extensive rill and gully formation in the hillslopes during the March 2015 storm event have been reported in this study in agreement with previous reports of arid zone hillslope responses to rainfall that have quantified the
10 contribution from gullies to be 50 to 80% of the overall sediment yield (Poesen et al., 2003).

The selective generation of debris flows within tributary catchments has been reported previously in Andean catchments (Colombo, 2010; Lauro et al., 2017). This selective activation might be explained by different coupling degrees between catchments and trunk valley (Fryirs et al., 2007; Mather and Stokes, 2017) or by the absence of the necessary rainfall amount to trigger debris flows in some catchments linked to the heterogeneous rainfall distribution of ENSO events (Colombo, 2010;
15 Cabr e et al., 2019). In that sense, the selective activation of a few catchments for El Elqui river valley was reported 130 km south of the study area (Vergara et al., 2018). Vergara et al. (2018) also highlights that the intensity of the 1-h peak storm precipitation had a low significance in the distribution of debris flow generation during the storms. The results of the logistic regression model in El Elqui river valley (Vergara et al., 2018) supports that the prediction of high discharge events does not depend on the antecedent precipitation (accumulated rainfall).

The entrainment of sediments from the drainage network during the March 2015 storm agrees with the topographical attributes of catchments that are used to identify significant debris flow generation. We have shown that the topographical attributes play a major role in the debris flow generation and distribution after extreme storms. Accordingly, most of the largest tributary catchments, with highly developed stream-networks and relatively low mean slopes, were activated during the March 2015 event. The large volumes of sediments stored in gullies and channels resulted in several debris flows during the storm
25 that yielded large volumes of sediment to the outlets (Fig. 10). In contrast, small and steep catchments, with low developed drainage network, store less volumes of sediments in the channels and thus during extreme storm events generate flows with lower sediment concentrations.

The altitude of zero-isotherm in this region of the Andes appears to greatly influence debris flow generation during high discharge events related to extreme precipitation events (Moreiras et al., 2018; Vergara et al., 2018). So, the high altitude of zero-isotherm during the March 2015 storm explains the abundant debris flow generation in the studied zone. In fact, greater area with effective water capture resultant in an widespread distribution of run-off in the head-watershed and higher volumes of water discharge downstream. However, altitudinal attributes of catchments are not identified as conditioning factors of the selective distributions of debris flow generation during the March 2015 event in the studied zone, because during this storm the zero-isotherm is above the maximum altitude of the topography.

Susceptibility assessment to debris flow generation must be evaluated in hydro-meteorological hazard studies for populated area (Wilford et al., 2004). In one sense, susceptibility of debris flow generation in the southern Atacama Desert is linked to the capacity of sediment-storage in a drainage network during the inter-storm period. Beside, susceptibility is linked to the percentage of the catchment over the altitude of zero-isotherm during the storm. The unusual altitude of zero-isotherm above the topography during the March 2015 storm explains the lack of similar sedimentary-behavior in the historical register and the extensive runoff of debris flows from the source of sediments. Considering debris flow susceptibility studies for a storm with a high zero-isotherm is relevant when considering its progressive increase of typical elevation of the zero-isotherm in Chile (Carrasco et al., 2005; Boiser et al., 2016) and in mountain areas worldwide (Mountain Research Initiative EDW Working Group, 2015).

10 5.2 The role of individual extreme storm events in erosion rates in the southern Atacama Desert

The occasional humid spells reported for the Mid-Holocene (8-4 ka) (Grosjean et al, 1997) or stormy conditions (Tiner et al., 2018) produced the necessary runoff to entrain sediment from the alluvial channels and hillslopes within tributary catchments of the Atacama Desert. This has been evidenced in the Holocene stratigraphy of the alluvial fans of El Huasco river valley by a number of cohesive debris flow layers and radiocarbon age, interpreted to result from episodic high-water discharge events during the last 8 ka BP (Cabr e et al., 2017). Therefore, stormy conditions and high sediment discharge at least occurred after 8 ka BP.

The increase of layers with coarse sediment in both lacustrine and marine archives during the last 5,500 years BP in Northern Chile are interpreted as high sediment discharge events associated with more recurrent extreme storms in the southern Atacama Desert (Rein et al., 2005; Tiner et al., 2018; Ortega et al., 2019). The recurrence time decreased from 1 event/210 yr towards 1 event/ 40 yr in the last 1,000 years BP (Ortega et al., 2019). Nevertheless, the increase of coarse-sediment layers could be showing more summer-austral storms, with high zero-isotherm altitude like the March 2015 storm. Therefore, this sedimentary record does not necessarily show changes of inter-decennial storm-return time linked to ENSO as interpreted by Ortega et al. (2019). A return of 116 years for the storms like March 2015 can be proposed as average for the southern Atacama Desert during the last 5,500 years based on Ortega et al. (2019). The return time proposed for the southern Atacama Desert is similar to the 100 years return time estimated by Houston (2006) in El Salado River a tributary of El Loa Valley in the Altiplano, where the influence of storms related to the warm phase of ENSO is low.

The role of extreme storm events in erosion rates should be considered only for data that encompass extensive areas or an exhaustive correlation between specific places because focused assessment might not be representative of a great magnitude storm like the March 2015 event. Quaternary erosion rates from concentration of Terrestrial Cosmogenic Nuclides in stream sediments of El Huasco river valley are reported in Aguilar et al. (2014). Their results presented denudation rates of 0.03-0.05 mm/yr and of 0.06-0.08 mm/yr, measured in sand and gravel grain-size fractions, respectively. The time period of denudation rates calculated by Aguilar et al. (2014) is between 20 ka for sand and 12 ka for gravels. The similarity between erosion rates during the last thousands of years (Aguilar et al., 2014) with those calculated during the last 8 Ma (Aguilar et al., 2011), suggests that long-term erosion rates remain unchanged (Aguilar et al., 2011).

An erosion rate of 10^{-2} mm/yr is calculated from this study based on the mean erosion of 1.3 mm for the whole study area in El Huasco river valley during the March 2015 storm and the return time of these kind of events from paleoclimatic record of 1 event each 100 years. This value agrees in order of magnitude with Holocene erosion rates calculated from Terrestrial Cosmogenic Nuclides concentration in stream sediments and Plio-Quaternary erosion rates calculated from missing volumes of incised deep-valley below Miocene pediments and paleo-valleys (0.03-0.08 mm/yr calculated by Aguilar et al. (2011) and Aguilar et al. (2014) respectively). These two independent proxies of long-term denudation show a great significance of erosion linked to extreme storms at scale of 10^6 - 10^4 years. The latter agree with a significant geomorphological contribution to millennial erosion rates of extreme storm events deduced from the comparison of erosion rates at different timescales in arid and semiarid mountainous chains (Kirchner et al., 2001; Kober et al., 2013; Carretier et al., 2013).

The limitations to study erosion associated with an individual storm event include the lack of pre-event high resolution topography (e.g. available digital elevation models; DEM's). The lack of detailed topographic surveys prior to the storm hinders the volume balance quantification from DEM's of difference (DOD's) to depict geomorphic change caused by gullies and rills on the hillslopes and erosion in the alluvial channels (e.g., Cavalli et al., 2017). Moreover, the calculated volumes from the debris flows deposits in the alluvial fans are the minimum values of erosion in the catchments because of sediment loss due to the river toe-cutting of alluvial fans. The sediment eroded and transported down-system by the trunk valley rivers signature might be recognized in suspended sediment concentrations measured at river gauges. Nevertheless, these records also underestimate the peak discharge associated with the storm because the gauging stations are commonly damaged by flash floods. Therefore, the volumes near to 1 million m^3 and mean erosion of 1.3 mm during the storm of March 2015 in El Huasco river valley should be considered with caution, and rather its order of magnitude should be considered.

6 Conclusions

The generation of debris flows in arid valleys of the southernmost Atacama Desert is controlled by the amount of available sediments stored within the catchments. Thus, the efficiency of catchments to store sediments depends in topographical attributes dictates whether the catchments are activated or not during extreme storm events. The sediment is stored during the inter-storm periods and therefore is susceptible to be transferred by debris flows when any extreme storm impacts the area. The alluvial channels are the main entrainment sediment zones during extreme storms whilst debris-supply from landslides on hillslope is not necessary for the debris flow generation, in these arid catchments during extreme storm events. The instantaneous increase in run-off during a storm and the entrainment of sediment has been associated with a high altitude of the zero-isotherm and the distribution of storm cells. Assessments of debris flow susceptibility in arid catchments of the Atacama Desert that incorporate as predictors the classification of catchment-clustering proposed here could be implemented easily, unlike alternative approaches to assessment that usually require exhaustive field-work observations.

Recently there has been some consensus that storms such as March 2015 in Atacama Desert occur on average every 100 years for the last 5,500 years (Ortega et al., 2019). Thus, the erosion rates associated with these storms are of the order of 10^{-2} mm/year in El Huasco river valley if we consider the erosion measurements after the March 2015 storm. The order of magnitude

of erosion is the same as the erosion rates calculated over the long term in the Huasco River valley (Aguilar et al., 2014). This indicates that these storms have a significant influence on the erosion and evolution of these arid fluvial systems of the Atacama Desert. It is these storms that denude effectively the coverage of sediments in the arid catchments of the southern Atacama Desert. However, the influence of the different surface processes in the preparation of the sediment cover before storms has yet to be characterized. New direct data, including quantitative geomorphological analysis of erosion, sedimentation and soil formation are required to quantify and have a knowledge of the rates, the routes, and the magnitudes of each process in the landscape evolution of the Atacama Desert.

Data availability. Morphometric and geological features of catchments

Competing interests. TEXT

10 *Acknowledgements.* This work is supported by the Basal Project of the Advanced Mining Technology Center financed by CONICYT Project AFB180004, Government of Chile. This work is based in the undergraduate thesis of V. Fredes (Universidad de Chile) and is part of the PhD thesis of A. Cabré supported by the Chilean Government funded by CONICYT + PAI/ Concurso nacional de tesis de doctorado en el sector productivo, 2017 Folio (T7817110003). We also acknowledge Planet Team grant (www.planet.com) given to A. Cabré. We gratefully acknowledge M. Lara and S. Sepúlveda contributions during the undergraduate thesis of V. Fredes and R. Riquelme for his
15 valuable contributions in the early stages of this manuscript.

References

- Aguilar, G., Carretier, S., Regard, V., Vassallo, R., Riquelme, R., and Martinod, J.: Grain size dependent ^{10}Be concentrations in alluvial stream sediment of the Huasco Valley, a semi-arid Andes region, *Quat. Geochron.*, 19, 163-172, 2014.
- Aguilar, G., Riquelme, R., Martinod, J., Darrozes, J., and Maire, E.: Erosion rates variability on landscape's transience state in the semiarid Chilean Andes. *Earth Surface Processes and Landforms* 36: 1736-1748, 2011.
- Aguilar, G., Riquelme, R., Martinod, J., Darrozes, J.: Role of climate and tectonics in the geomorphologic evolution of the Semiarid Andes between 27-32°S. *Andean Geology* 40(1): 79-101, 2013.
- Aguilar, G.: Érosion et transport de matière sur le versant occidental des Andes semiàrides du Nord du Chili (27 -32S): d'une approche à grande échelle temporelle et spatiale, jusqu'à l'évolution quaternaire d'un système fluvial. Thèse doctoral, Université de Toulouse, 204 p., Toulouse, France, 2010.
- Anderson, S. W., Anderson, S. P., and Anderson, R. S.: Exhumation by debris flows in the 2014 Colorado front range storm. *Geology*, 43 (5), 391-394, doi:10.1130/G36507.1, 2015.
- Barrett, B.S., Campos, D.A., Veloso, J.V., Rondanelli, R.: Extreme temperature and precipitation events in March 2015 in central and northern Chile. *Journal of Geophysical Research, Atmospheres*, 121 (9): 4563-4580, 2016.
- Berti, M., Martina, M.L.V., Franceschini, S., Pignone, S., Simoni, A., and Pizziolo, M.: Probabilistic rainfall thresholds for landslide occurrence using a Bayesian approach. *J. Geophys. Res.*, 117, F04006, 2012.
- Boisier, J.P., Rondanelli, R., Garreaud, R.D., and Muñoz, F.: Anthropogenic and natural contributions to the Southeast Pacific precipitation decline and recent megadrought in Central Chile. *Geophys. Res. Lett.* 43 (1), 413-421, 2016.
- Bovis, M., and Jakob, M.: The role of debris supply conditions in predicting debris flow activity. *Earth surface processes and landforms* 24, n. 11, p. 1039-1054, 1999.
- Box, G.E.P., Hunter, W.G., and Hunter, J.S.: *Statistics for Experimenters: An Introduction to Design, Data Analysis and Model Building*. John Wiley and Sons Inc., New York, USA, ISBN-13: 9780471093152, Pages: 653, 1978.
- Bozkurt, D., Rondanelli, R., Garreaud, R., and Arriagada, A.: Impact of warmer eastern tropical Pacific SST on the March 2015 Atacama floods. *Mon. Wea. Rev.*, 144, 4441-4460, 2016.
- Cabré, A., Aguilar, G., and Riquelme, R.: Holocene evolution and geochronology of a semiarid fluvial system in the western slope of the Central Andes: AMS ^{14}C data in El Tránsito River Valley, Northern Chile. *Quaternary International*, 438, 20-32, 2017.
- Cabré, A., Aguilar, G., and Colombo, F.: Abanicos aluviales tributaries en un valle fluvial desarrollado en un context árido. *Andes de Chile a los 29°S*. *Geogaceta*, 66, 2019.
- Cabré, A., Aguilar, G., Mather, A.E., Fredes, V., and Riquelme, R.: Tributary-junction alluvial fan response to an ENSO rainfall event at El Huasco river watershed, northern Chile. Submitted to *Progress in Physical Geography*.
- Campbell, D. and Church, M.: Reconnaissance sediment budgets for Lynn Valley, British Columbia: Holocene and contemporary time scales. *Can. J. Earth Sci.* 40, 701-713, doi:10.1139/E03-012, 2003.
- Cavalli, M., Goldin, B., Comiti, F., Brardinoni, F., and Marchi, L.: Assessment of erosion and deposition in steep mountain basins by differencing sequential digital terrain models. *Geomorphology* 291, Pages 4-16. <https://doi.org/10.1016/j.geomorph.2016.04.009>, 2017.
- Carrasco, J.F., Casassa, G., and Quintana, J.: Changes of the 0°C isotherm and the equilibrium line altitude in central Chile during the last quarter of the 20th century. *Hydrological Sciences–Journal–des Sciences Hydrologiques*, 50(6), 2005.

- Carretier, S., Regard, V., Vassallo, R., Aguilar, G., Martinod, J., Riquelme, R., Pepin, E., Charrier, R., Herail, G., Farias, M., Guyot, J. L., Vargas, G., and Lagane C.: Slope and climate variability control of erosion in the Andes of Central Chile. *Geology* (2013), DOI:10.1130/G33735.1, 2013.
- Carretier, S., Regard, V., Vassallo, R., Aguilar, G., Martinod, J., Riquelme, R., Christophoul, F., Charrier, R., Gayer, E., Farías, M., Audin, L.,
5 and Lagane, C.: Differences in ^{10}Be concentrations between river sand, gravel and pebbles along the western side of the central Andes. *Quaternary Geochronology* 27: 33-51. DOI: 10.1016/j.quageo.2014.12.002, 2015.
- Carretier, S., Tolorza, V., Regard, V., Aguilar, G., Bermúdez, M.A., Martinod, J., Guyot, J.L., Hérail, G., and Riquelme, R.: Review of erosion dynamics along the major N-S climatic gradient in Chile and perspectives. *Geomorphology* 300, 45-68. 2018.
- Coe, J.A., Kinner, D.A., and Godt, J.W.: Initiation conditions for debris flows generated by runoff at Chalk Cliffs, central Colorado. *Geomorphology* 96, 270–297, 2008.
10
- Colombo, F.: Sedimentología. Del proceso físico a la Cuenca sedimentaria (Ed. Alfredo Arche), Textos Universitarios 46, CSIC, 2010.
- Coppus, R., and Imeson, A.C.: Extreme events controlling erosion and sediment transport in a semi-arid sub-andean valley. *Earth Surface Processes and Landforms*, 27, 1365-1375, 2002.
- Davis, J.: *Statistics and Data Analysis in Geology*, 3rd Edition. Wiley. ISBN: 978-0-471-17275-8. 656 pages, 2002.
- 15 Favier, V., Falvey, M., Rabatel, A., Praderio, E., and López, D.: Interpreting discrepancies between discharge and precipitation in high-altitude area of Chile's Norte Chico region (26–32S). *Water Resour. Res.* 45, 1–20, 2009.
- Fredes, V.: Evaluación estadística de factores generadores de flujos de detritos durante el evento del 25 de Marzo de 2015 en la cuenca del valle del Huasco, Comuna de Vallenar, III Región de Atacama. Memoria para optar al Título de Geólogo, Universidad de Chile, 62 pag., 2016.
- 20 Fryirs, K.A., Brierley, G.J., Preston, N.J., and Kasai, M.: Buffers, barriers and blankets: the (dis)connectivity of catchment-scale sediment cascades. *Catena* 70, 49–67. Doi:10.1016/j.geomorph.2009.11.015, 2007.
- Gascoïn, S., Kinnard, C., Ponce, R., Lhermitte, S., Macdonell, S., and Rabatel, A.: Glacier contribution to streamflow in two headwaters of the Huasco River, dry Andes of Chile. *Cryosphere* 5, 1099–1113, 2011.
- González de Vallejo, L.: *Ingeniería Geológica*. Pearson: Prentice-Hall, Madrid, 715 pag., 2002.
- 25 Horton, R.: *Erosional Development of Streams and their Drainage Basins; hydrophysical approach to quantitative Morphology*. Bulletin of the Geological Society of America, Vol. 56, Pag. 275-370, 1945.
- Houston, J.: Variability of precipitation in the Atacama Desert: Its causes and hydrological impact, *Int. J. Climatol.*, 26, 2181–2198, 2006.
- Howard, A.D., and Kerby, G.: Channel changes in badlands: *Geological Society of America Bulletin*, v. 94, p. 739–752, 1983.
- Jordan, T.E., Herrera, C., Godfrey, L.V., Colucci, S.J., Gamboa, C., Urrutia, J., González, G., and Paul, J.F.: Isotopic characteristics and
30 paleoclimate implications of the extreme precipitation event of March 2015 in northern Chile. *Andean Geology*, 46 (1), 1-31, 2019.
- Kean, J.W., McCoy, S.W., Tucker, G.E., Staley, D.M., and Coe, J.A.: Runoff-generated debris flows: Observations and modeling of surge initiation, magnitude, and frequency, *J. Geophys. Res. Earth Surf.*, 118, 2190–2207, doi:10.1002/jgrf.20148, 2013.
- Kirchner, J.W., Finkel, R.C., Riebe, C.S., Granger, D.E., Clayton, J.L., King, J.G., and Megahan, W.F.: Mountain erosion over 10 yr, 10 k.y., and 10 m.y. time scales. *Geology*, 29 (7), 591-594, 2001.
- 35 Kober, F., Hippe, K., Salcher, B., Ivy-Ochs, S., Kubik, P.W., Wacker, L., and Hähnen, N.: Debris-flow-dependent variation of cosmogenically derived catchment-wide denudation rates. *Geology*, 40 (10), 935-938, 2012.
- Lauro, C., Moreiras, S.M., Junquera, S., Vergara, I.P., and Toural, R.: Summer rainstorm associated with a debris flow in the Amarilla gully affecting the international Agua Negra Pass (30°20'S), Argentina. *Environmental Earth Sciences*; 76 (5), 1-12, 2017.

- Levy, J, and Varela, J.: Análisis multivariable para las ciencias sociales. Prentice Hall, Madrid. 862 p, 2003.
- Maldonado, A., and Villagrán, C.: Climate variability over the last 9900 cal yr BP from a swamp forest pollen record along the semi-arid coast of Chile. *Quaternary Research* 66, 246–258, 2006.
- Martel-Cea, A., Maldonado, A., Grosjean, M., Alvial, I., de Jong, R., Fritz, S. C., and von Gunten, L.: Late Holocene environmental changes as recorded in the sediments of high Andean Laguna Chepical, Central Chile (32°S; 3050 m a.s.l.). *Paleogeogr. Palaeoclimatol. Palaeocol.* <http://dx.doi.org/10.1016/j.palaeo.2016.08.003>, 2016.
- Mather, A.E. and Stokes, M.: Bedrock structural control on catchment-scale connectivity and alluvial fan processes, High Atlas Mountains, Morocco In Ventra, D. and Clarke, L. E. (eds.) *Geology and Geomorphology of Alluvial and Fluvial Fans: Terrestrial and Planetary Perspectives*. Geological Society, London, Special Publications, 440, doi:10.1144/SP440.15, 2017.
- 10 Melton, M.: An analysis of the relation among elements of climate, surface properties and geomorphology. No. CU-TR-11. Columbia University, New York, 1957.
- Melton, M.: The Geomorphic and Paleoclimatic Significance of Alluvial Deposits in Southern Arizona. *The Journal of Geology*. Volume 73(1), 1-38, 1965.
- Moreiras, S.M., Pont, I.V., and Araneo, D.: Were merely storm-landslides driven by the 2015-2016 Niño in the Mendoza River valley? *Landslides*. <https://doi.org/10.1007/s10346-018-0959-3>, 2018.
- 15 Mountain Research Initiative EDW Working Group: Elevation-dependent warming in mountain regions of the world. *Nature Climate Change* volume 5, 424–430, <https://doi.org/10.1038/nclimate2563>, 2015.
- Nicoletti, P.G., and Sorriso-Valvo, M.: Geomorphic controls of the shape and mobility of rock avalanches. *Geol. Soc. Am. Bull.* 103, 1365–1373, 1991.
- 20 Ortega, C., Vargas, G., Rutllant, J.A., Jackson, D., and Méndez, C.: Major hydrological regime change along the semi-arid western coast of South America during the early Holocene. *Quaternary Research*, 78, 512-527, 2012.
- Ortega, C., Vargas, G., Rojas, M., Rutllant, J.A., Muñoz, P., Lange, C.B., Pantoja, S., Dezileau, L., and Ortlieb, L.: Extreme ENSO-driven torrential rainfalls at the southern edge of the Atacama Desert during the late Holocene and their projection into the 21st century. *Global and planetary change*, 175, 226-237, 2019.
- 25 Ortlieb, L.: El Niño events and rainfall episodes in the Atacama desert: the record of the last two centuries in Eaux, glaciers and changements climatiques dans les Andes tropicales, Éditeurs: Ribstein, P., Francou, B., Coudrain-Ribstein, A., Mourguiart, P., *Bulletin de l'institute français d'études Andines*, 24(3), 519-537, 1995.
- Ortlieb, L.: Las mayores precipitaciones históricas en Chile central y la cronología de eventos ENOS en los siglos XVI-XIX. *Revista Chilena de Historia Natural*, 67, 463-485, 1994.
- 30 Planet Team: Planet Application Program Interface: In *Space for Life on Earth*. San Francisco, CA. <https://api.planet.com>, 2017.
- Poesen, J., Nachtergaele, J., Verstraeten, G., and Valentin, C.: Gully erosion and environmental change: importance and research needs. *Catena*, Vol: 50, Issue: 2, Page: 91-133, 2003.
- Rein, B., Lückge, A., Reinhardt, L., Sirocko, F., Wolf, A., and Dullo, W.C.: El Niño variability off Peru during the last 20,000 years. *Paleoceanography*, 20, PA4003, doi:10.1029/2004PA001099, 2005.
- 35 Roda-Boluda, D., D'Arcy, M., McDonald, J., and Whittaker, A.: Lithological controls on hillslope sediment supply: insights from landslide activity and grain size distributions. *Earth Surf. Process. Landforms* 43, 956–977. DOI: 10.1002/esp.4281, 2018

- Rossel, K., Aguilar, G., Salazar, E., Martinod, J., Carretier, S., Pintgo, L., Cabré, A.: Chronology of Chilean Frontal Cordillera building from geochronological, stratigraphic and geomorphological data insights from Miocene intramontane-basin deposits. *Basin Research* 30, issue S1: 289-310, 2018.
- Salazar, E., Coloma, F., and Creixell, C.: *Geología del área El Tránsito-Lagunillas, Región de Atacama*. Servicio Nacional de Geología y Minería, Carta Geológica de Chile, Serie Geología Básica 149, 1 mapa escala 1:100.000, 2013.
- Selby, M.J.: *Hillslope Materials and Processes*. second ed. Oxford University Press, Oxford, 1993.
- Sepúlveda, S.A., and Padilla, C.: Rain-induced debris and mudflow triggering factors assessment in the Santiago cordilleran foothills, Central Chile. *Nat Hazards* (2008) 47: 201. <https://doi.org/10.1007/s11069-007-9210-6>, 2008.
- Stokes, M., and Mather, A.M.: Controls on modern tributary-junction alluvial fan occurrence and morphology: high Atlas Mountains, Morocco. *Geomorphology* 248, 344-362, 2015.
- Strahler, A.: Dimensional analysis applied to fluvially eroded landforms. *Geol Soc Am Bull* 69: 279-99, 1958.
- Tarr, R.S.: Erosive agents in the arid regions. *The American Naturalist*, 24 (281), 455-459, 1890.
- Tiner, R.J., Negrini, R.M., Antinao, J. L., McDonald, E., and Maldonado, A. Geophysical and geochemical constraints on the age and paleoclimate implications of Holocene lacustrine cores from the Andes of central Chile. *Journal of Quaternary Science*, 33(2), 150-165, 2018.
- Vargas, G., Rutllant, J., and Ortlieb, L.: ENSO tropical-extratropical climate teleconnections and mechanisms for Holocene debris flows along the hyperarid coast of western South America (17°-24°S). *Earth and Planetary Science Letters* 249, 467-483, 2006.
- Vargas, G., Pérez, S., and Aldunce, P.: Aluviones y resiliencia en Atacama. *Construyendo saberes sobre riesgos y desastres*. Ed. Social Ediciones, 363, 2018.
- Veit, H.: Southern Westerlies during the Holocene deduced from geomorphological and Pedological Studies in the Norte Chico, Northern Chile (27-33°S). *Palaeogeogr. Palaeoclimatol. Palaeoecol.* 123, 107-119, 1996.
- Vergara Dal Pont, I.P., Santibañez-Ossa, F.A., and Araneo, D.: Determination of probabilities for the generation of high-discharge flows in the middle basin of Elqui River, Chile. *Nat Hazards* (2018) 93: 531. <https://doi.org/10.1007/s11069-018-3313-0>, 2018.
- Wilcox, A.C., Escauriaza, C., Agredano, R., Mignot, E., Zuazo, V., Otarola, S., Castro, L., Gironas, J., Cienfuegos, R., and Mao, L.: An integrated analysis of the March 2015 Atacama floods. *Geophys. Res. Lett.*, 43, 8035–8043, doi:10.1002/2016GL069751, 2016.
- Wilford, D., Sakals, M., Innes, J., Sidle, R., and Bergerud, W.: Recognition of debris flow, debris flood and flood hazard through watershed morphometrics. *Landslides*, vol.1, Issue 1, p.61-66, 2004.

Table 1. Table that summarizes the percentages of catchments prone to generate debris flows and presents thresholds of topographic attributes that contribute within each factor.

Size Factor	Catchments (%)	Area (km ²)	Length (km)	Strahler Order
0.05-0.25	18 (4 of 22)	<1	<2	1-2
0.25-0.75	39 (30 of 74)	1-7	2-5	2-4
0.75-1.50	57 (13 of 23)	>7	>5	4-6
Relief Factor	Catchments (%)	Slope (°)	Melton (km/km ²)	Gradient (km/km)
1.75-2.00	9 (1 of 11)	>30	>1.1	>0.6
1.75-1.25	33 (15 of 46)	1-7	1.1-0.7	0-6-0.4
1.25-0.25	50 (31 of 62)	<26	<0.7	<0.4

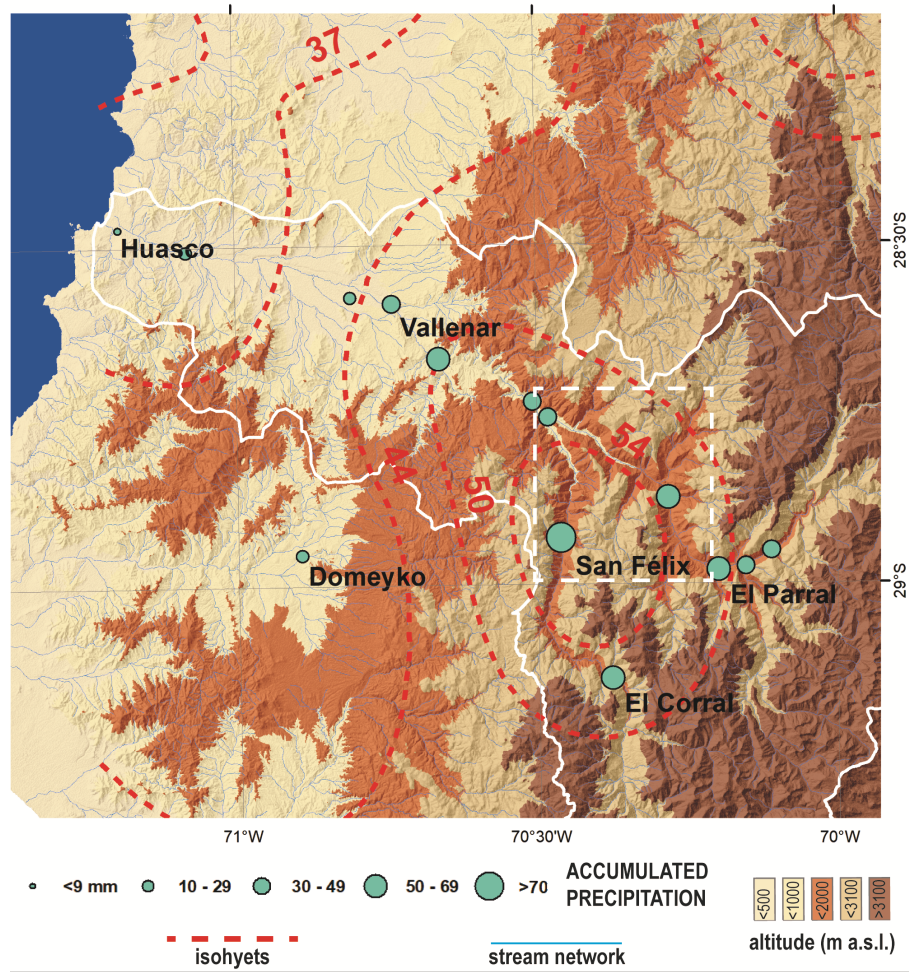


Figure 1. Topography extracted from a Digital Elevation Model Courtesy NASA/JPL-Caltech with a nominal spatial pixel resolution of 30 x 30 m (<https://asterweb.jpl.nasa.gov/gdem.asp>) and modeled hydrology of the Huasco River Valley. Dotted red lines show the isohyets of daily accumulated rains during the March 23–26th storm by kriging interpolation of meteorological data from Dirección General de Aguas - Chile. Cyan points show the accumulated rainfall in each meteorological station during the March 2015 storm. Dashed-line white box show the studied region.

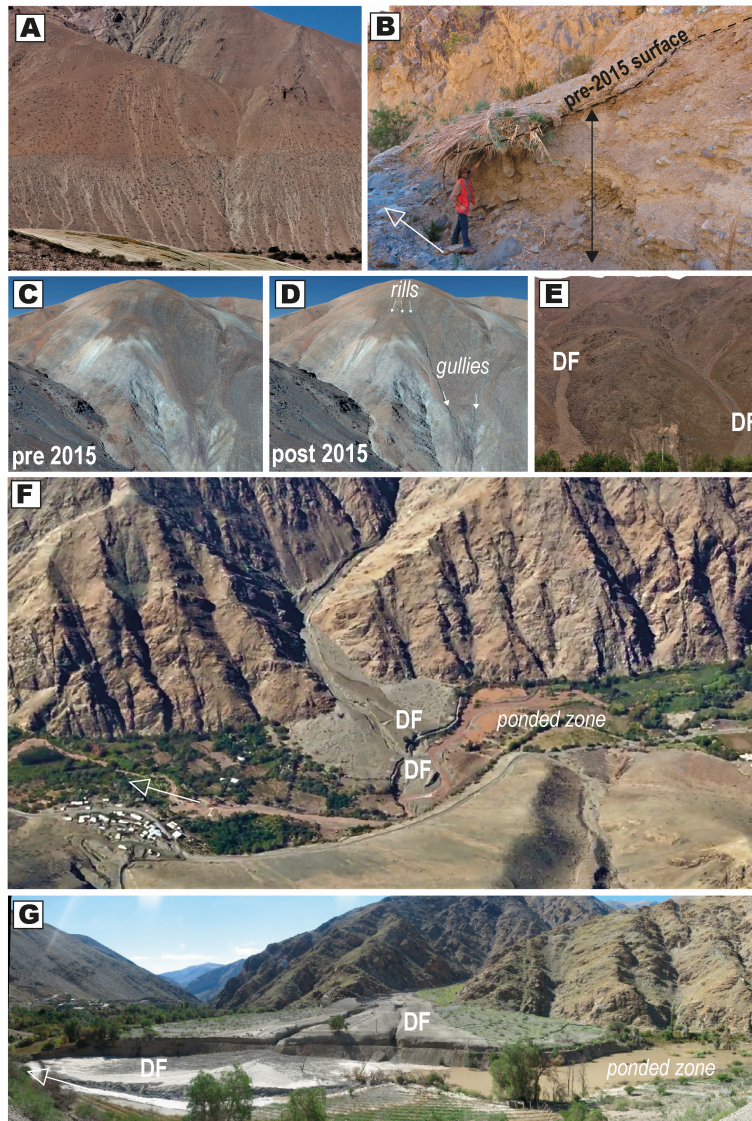


Figure 2. (A) Field evidence of high-density rill formation during the March 2015 storm on hillslopes of the Huasco River Valley. (B) Example of a deeply incised alluvial channel within a tributary catchment. Dashed line indicates pre-March 2015 storm surface with covered vegetation lying down overlain by a 30 cm layer of debris flows (DF) deposit triggered by the storm in and subsequently incised by more diluted flows. Person for scale is 180 cm tall. White arrow indicates the flow direction downwards. (C) and (D) indicate pre and post landscape configuration showing rills, gullies and debris flows. (E) Debris flows (DF) with lateral levees deposited within the tributary catchment alluvial channels with subsequent incision. (F) Oblique aerial view of debris flows deposits on a tributary junction alluvial fan and the upstream zone which was ponded by the damming with the distal depositional lobe. G. Front view of the tributary-junction alluvial fan of F).

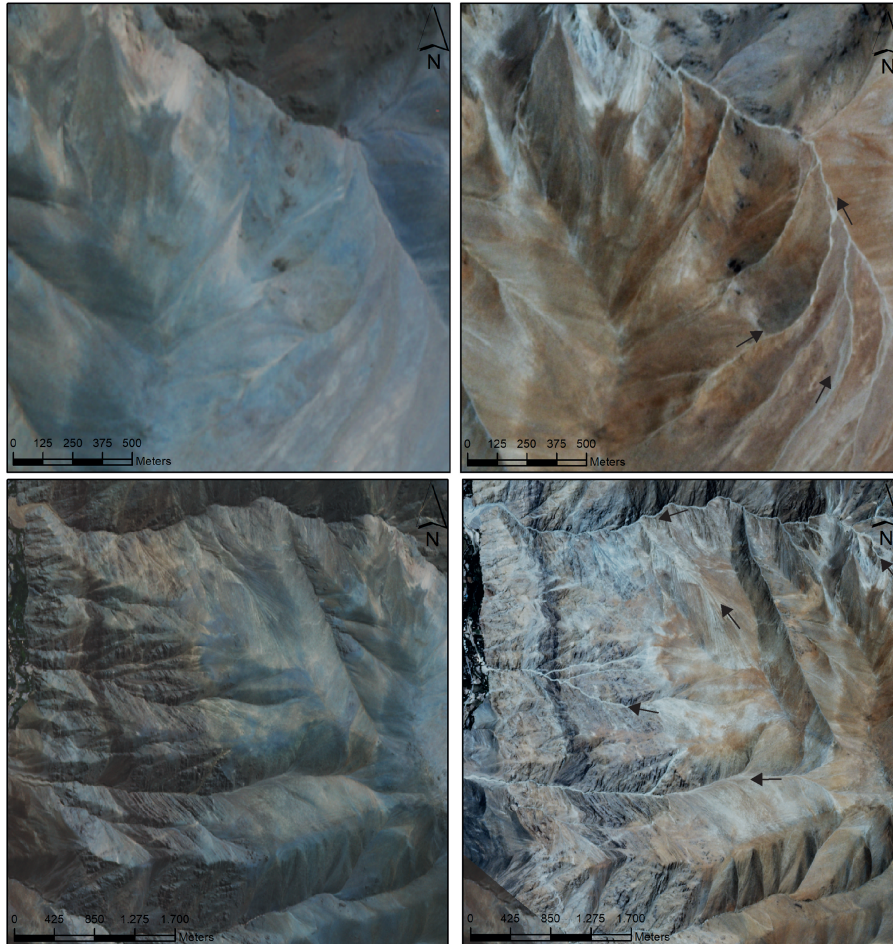


Figure 3. Optical imagery retrieved from Planet Team (2017) before and after March 2015 storm. Left images are before the March 2015 storm and right images are after. Arrows indicates different physical evidence of erosion processes due to the event and gully presence after March 2015 storm. The general color tone change merely indicates different sun illumination.

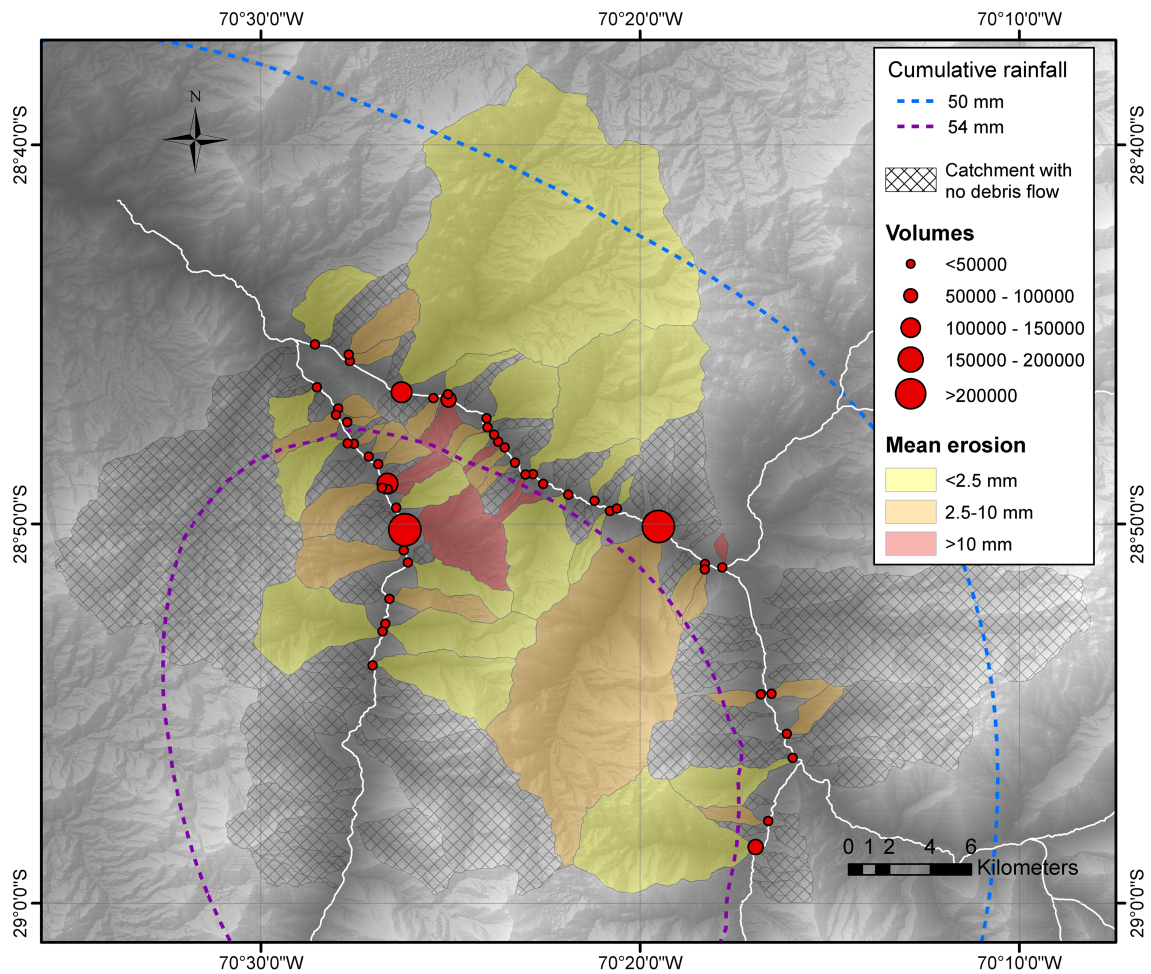


Figure 4. Distribution and volumes of debris flow deposits during the March, 2015 storm event in El Huasco river valley and identification of catchments where these flows were generated. Map shows the distribution of calculated mean erosion of tributary catchments and isohyets of accumulated rains by kriging interpolation of meteorological data during the storm. Topography extracted from a Digital Elevation Model Courtesy NASA/JPL-Caltech with a nominal spatial pixel resolution of 30 x 30 m (<https://asterweb.jpl.nasa.gov/gdem.asp>). The area of the map is the Dashed-line white box of Fig. 1

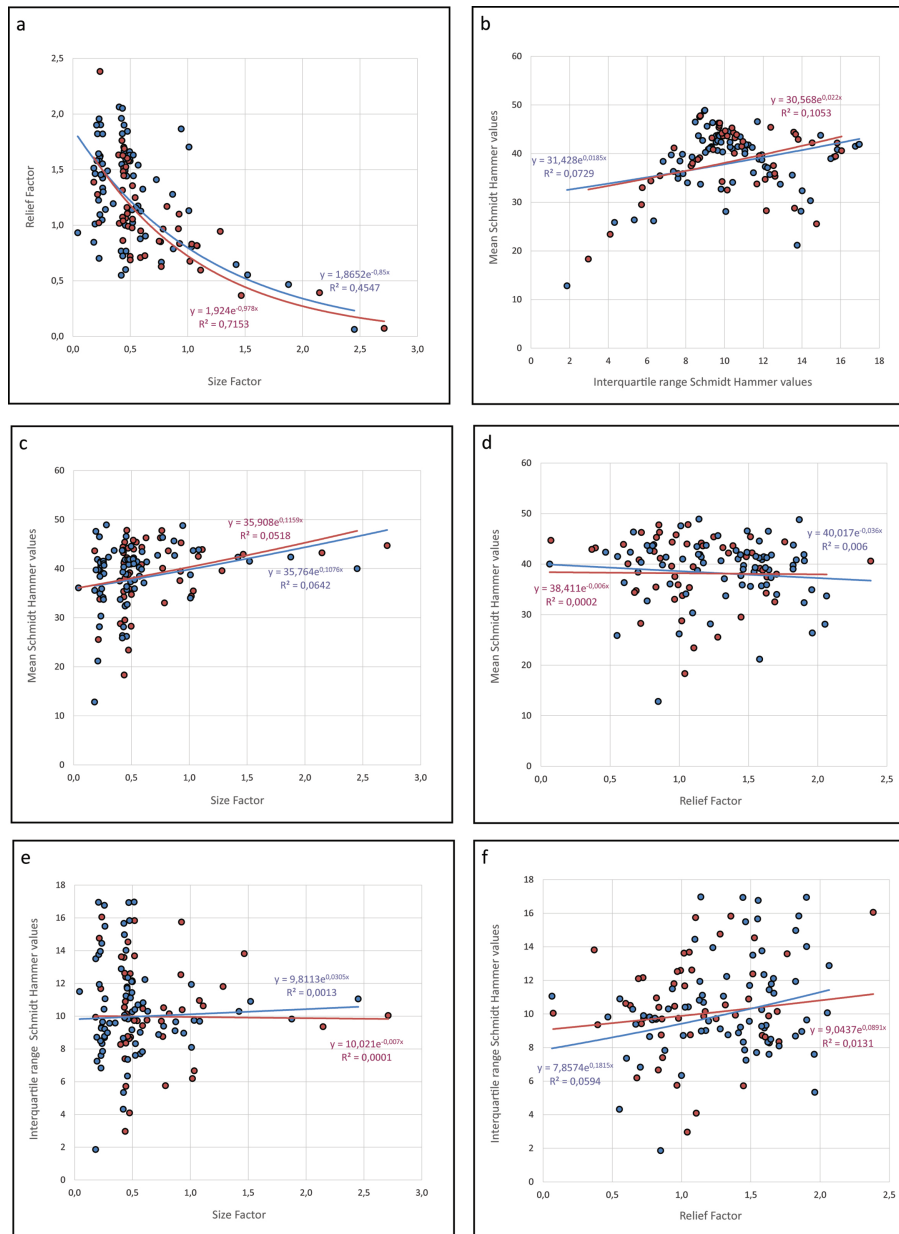


Figure 5. Graphics show relationship between different studied factors in catchments with debris flow generation in red and non-generation in blue. (a) Relationship between Size Factor and Relief Factor. (b) Relationship between Mean and Interquartile range of Schmidt Hammer values. (c) Relationship between Mean Schmidt Hammer values and Size Factor. (d) Relationship between Mean Schmidt Hammer values and Relief Factor. (e) Relationship between Interquartile range of Schmidt Hammer values and Size Factor. (f) Relationship between Interquartile range of Schmidt Hammer values and Relief Factor. In all graphics dotted box indicate ranges with enough data to statistically analysis (greater than 5 catchments for range).

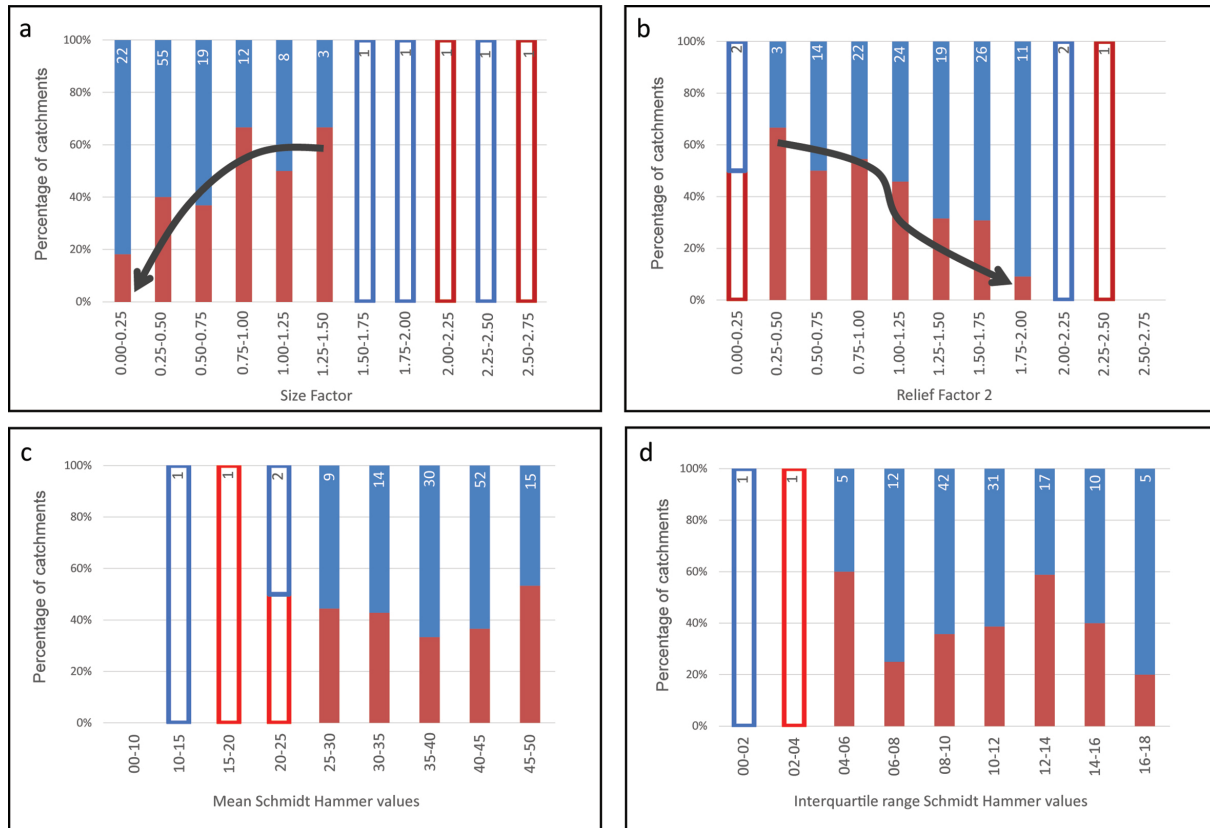


Figure 6. Histograms with the relative percentage of catchments with debris flow generation in red and non-generation in blue considering range of values for: (a) Size Factor, (b) Relief Factor, (c) normalized mean Schmidt Hammer values and (d) normalized interquartile range Schmidt Hammer values. Each bar includes a number indicating the quantity of analyzed catchments. Open bars indicate ranges without enough data to justify a statistical analysis (fewer than 5 catchments for range). Arrows indicate a trend in the histograms

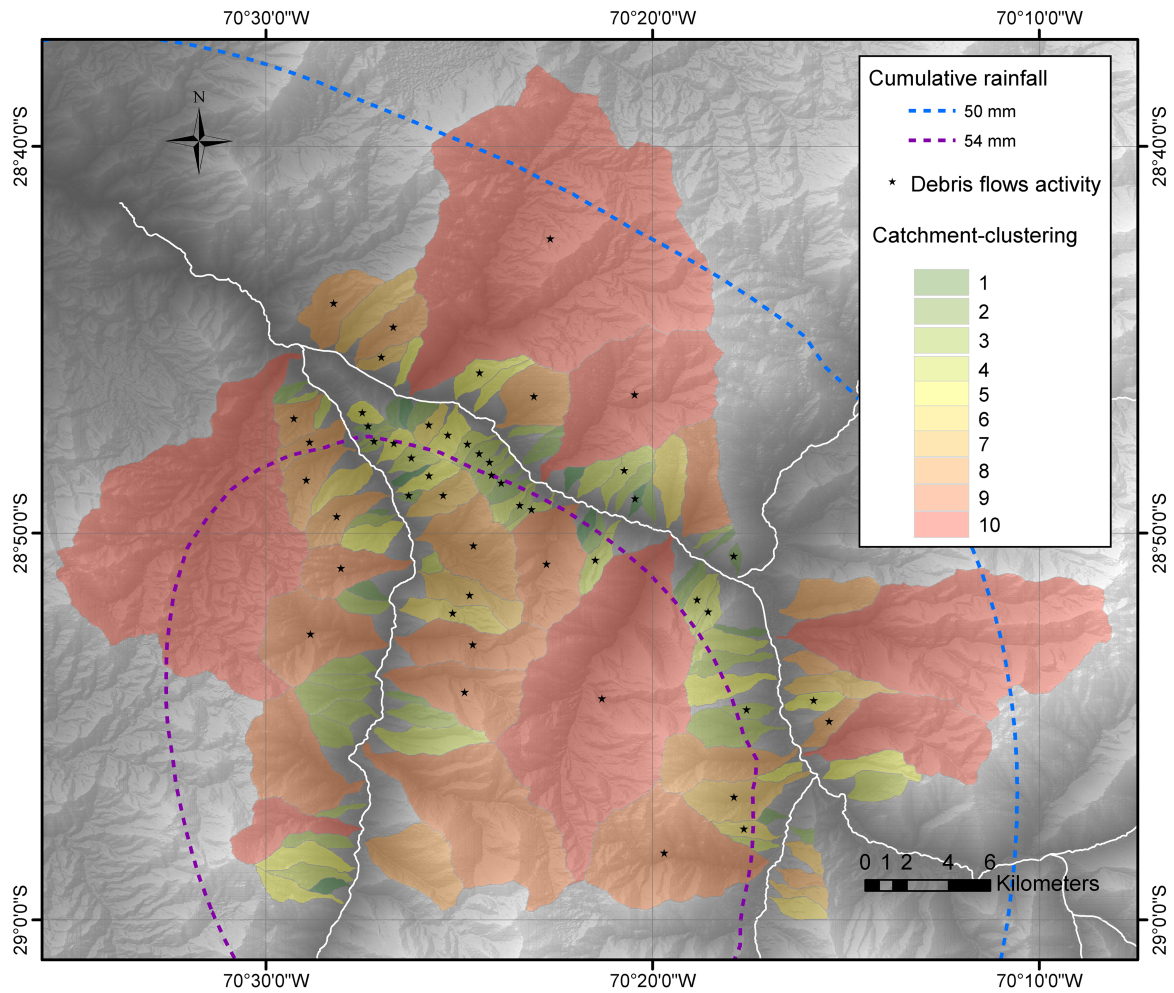


Figure 7. Map of the normalized classification of catchment-clustering considering the six topographic attributes (Area, Length, Strahler Order, Slope, Melton ratio and Relief ratio) involved in conditioning-factor of debris flow generation. Topography extracted from a Digital Elevation Model Courtesy NASA/JPL-Caltech with a nominal spatial pixel resolution of 30 x 30 m (<https://asterweb.jpl.nasa.gov/gdem.asp>).

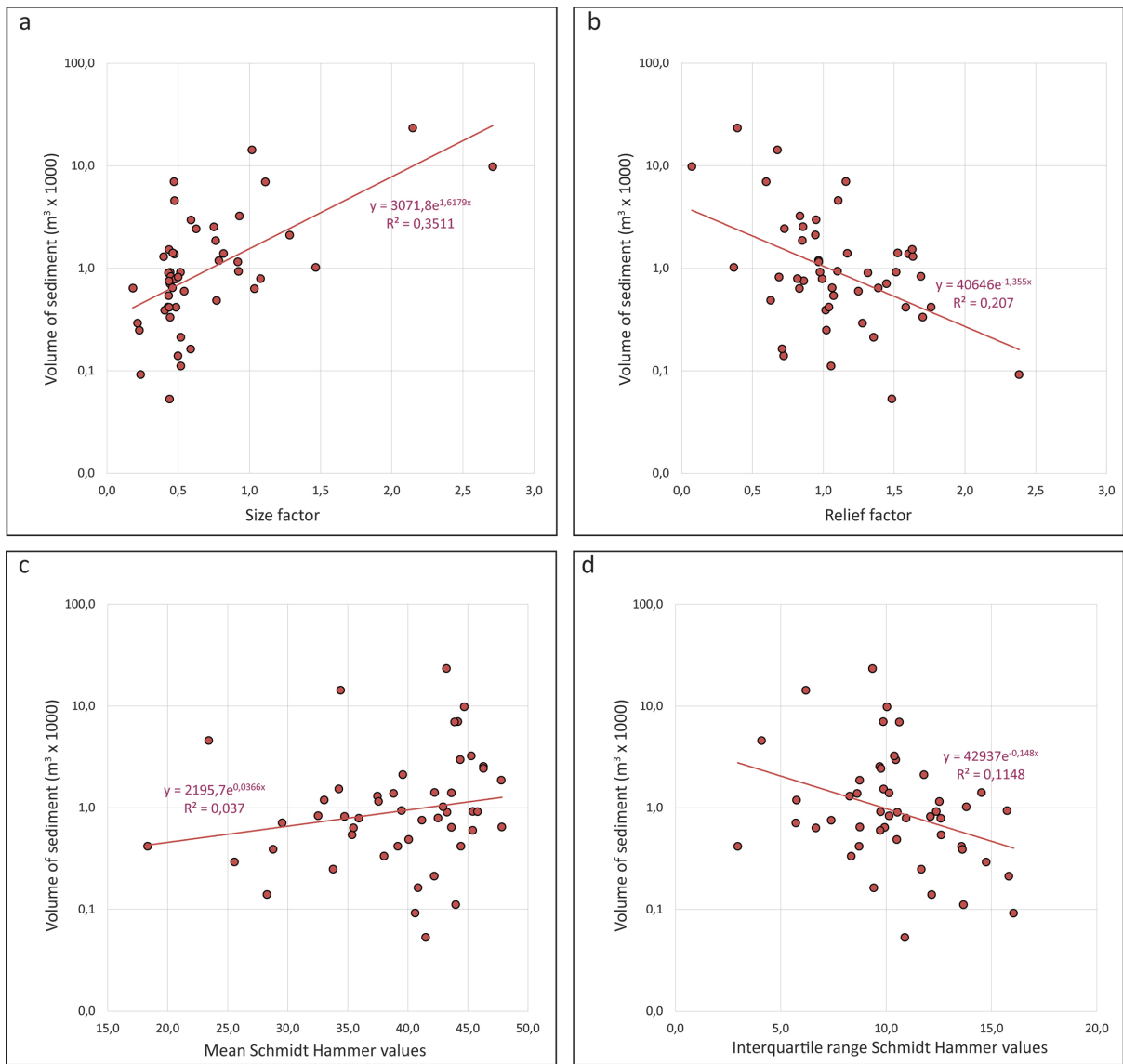


Figure 8. Graphics showing the relationship between different studied factors in catchments with sediment volumes of debris flow deposits. (a) Relationship between Size Factor and sediment volumes. (b) Relationship between Relief Factor and sediment volumes. (c) Relationship between Mean Schmidt Hammer values and sediment volumes. (d) Relationship between interquartile range Schmidt Hammer values and sediment volumes.

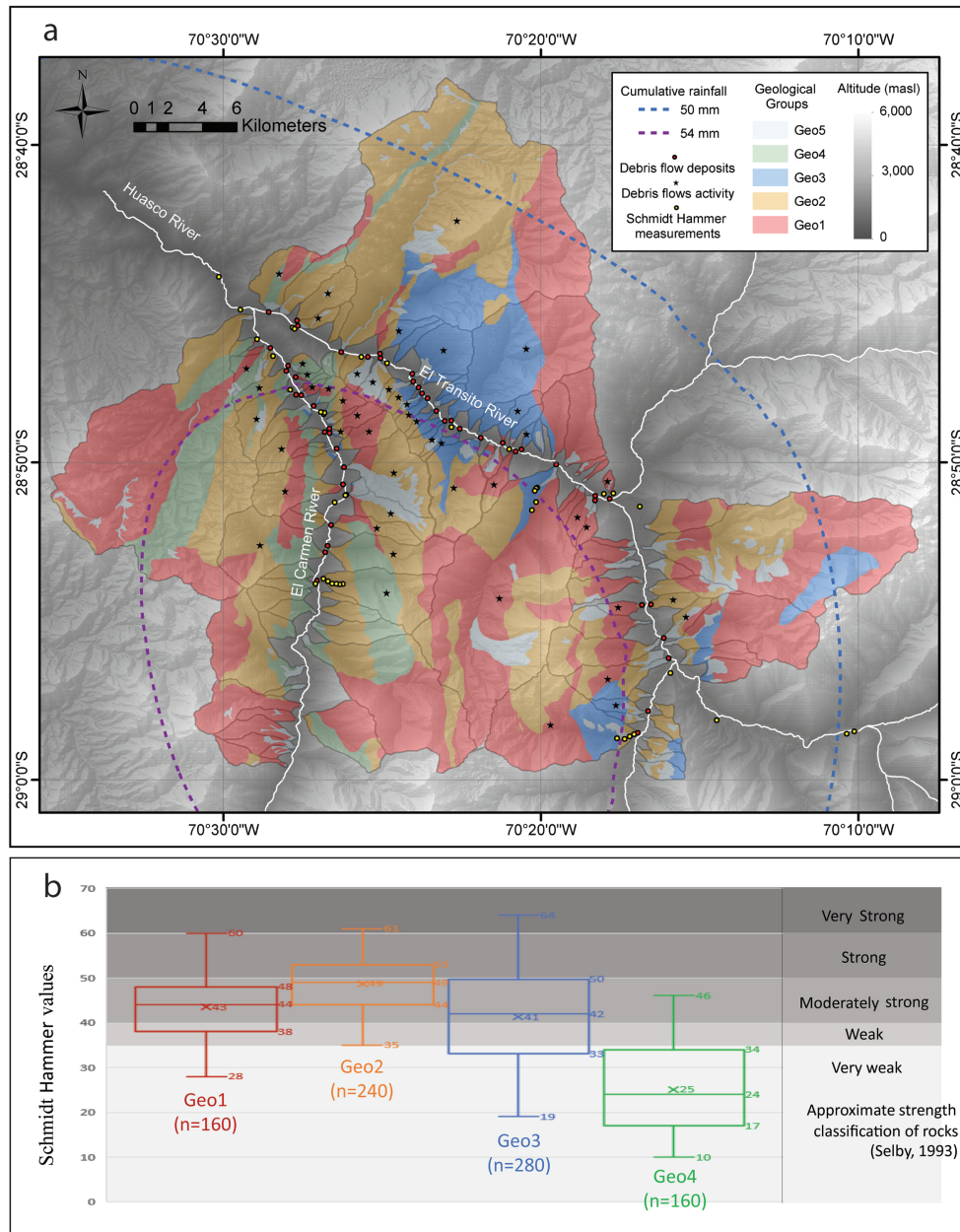


Figure 9. (a) Map that shows the distribution of Geological Groups defined in El Huasco river valley after Salazar et al. (2013) with the location of Schmidt Hammer stations. The map includes the distribution of debris flow deposits during March 2015 and isohyets of accumulated rains created by kriging interpolation of meteorological data during the storm. Topography extracted from a Digital Elevation Model Courtesy NASA/JPL-Caltech with a nominal spatial pixel resolution of 30 x 30 m (<https://asterweb.jpl.nasa.gov/gdem.asp>). (b) Whisker and box plots of Schmidt Hammer values for geological groups of the studied zone where n represent the number of measurements. Graphic show maximum, minimum and mean values for each geological group and also the values of 75th, 50th and 25th percentiles for each group. Graphic show the approximate strength classification of rocks by Schmidt Hammer values after Selby (1993).

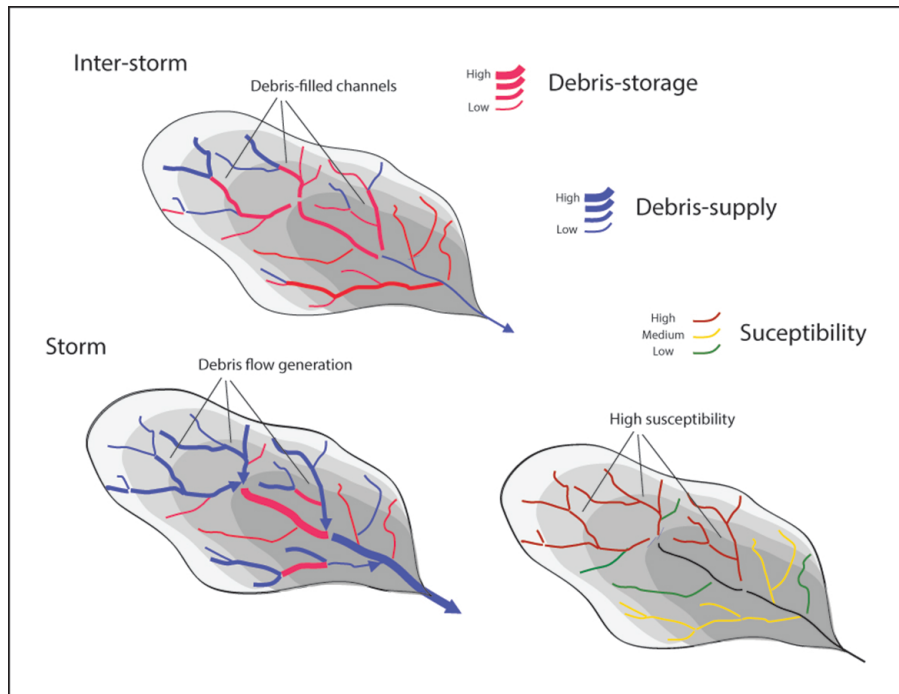


Figure 10. Conceptual model of the relation between hydraulic capacity during the intense long-lived rainfalls of an extraordinary storm and debris storage at previous time span that explain different levels of debris flow susceptibility depending on catchment topography.